ESMO GOOD SCIENCE BETTER MEDICINE BEST PRACTICE

ANNALS OF ONCOLOGY driving innovation in oncology

ORIGINAL ARTICLE

B-cell infiltration is associated with survival outcomes following programmed cell death protein 1 inhibition in head and neck squamous cell carcinoma

N. Gavrielatou[1,2], E. Fortis[3], A. Spathis[4], M. Anastasiou[1], P. Economopoulou[1], G. R. P. Foukas[4], I. M. Lelegiannis[1], S. Rusakiewicz[3], I. Vathiotis[2], T. N. Aung[2], S. Tissot[3], A. Kastrinou[1], I. Kotsantis[1], E. M. Vagia[1], I. Panayiotides[4], D. L. Rimm[2], G. Coukos[3], K. Homicsko[3], P. Foukas[4] & A. Psyrri[1]*

[1]Department of Internal Medicine, Section of Medical Oncology, Attikon University Hospital, National Kapodistrian University of Athens, Athens, Greece; [2]Department of Pathology, Yale University School of Medicine, New Haven, USA; [3]Ludwig Institute for Cancer Research, University Hospital of Lausanne (CHUV), Lausanne, Switzerland; [4]Department of Pathology, Attikon University Hospital, National Kapodistrian University of Athens, Athens, Greece

Available online 28 December 2023

Background: Programmed cell death protein 1 (PD-1) axis blockade has become the mainstay in the treatment of recurrent and/or metastatic (R/M) head and neck squamous cell cancer (HNSCC). Programmed death-ligand 1 (PD-L1) is the only approved biomarker for patient selection; however, response rate is limited even among high expressors. Our primary objective was to investigate the association of immune cell-related biomarkers in the tumor and tumor microenvironment with PD-1 checkpoint inhibitors' outcomes in patients with R/M HNSCC.

Patients and methods: NCT03652142 was a prospective study in nivolumab-treated platinum-refractory R/M HNSCC, aiming to evaluate biomarkers of response to treatment. Tumor biopsies and blood samples were collected from 60 patients at baseline, post-treatment, and at progression. Immune cells in the tumor and stromal compartments were quantified by immunofluorescence using a five-protein panel (CD3, CD8, CD20, FoxP3, cytokeratin). Tertiary lymphoid structures (TLSs), PD-L1 expression, and peripheral blood immune cell composition were also evaluated for associations with outcome. Our findings were validated by gene set enrichment analysis (GSEA) messenger RNA *in situ* expression data from the same patients, for B-cell- and TLS-associated genes.

Results: High pre-treatment density of stromal B cells was associated with prolonged progression-free survival (PFS) ($P = 0.011$). This result was validated by GSEA, as stromal enrichment with B-cell-associated genes showed association with response to nivolumab. PD-L1 positivity combined with high B-cell counts in stroma defined a subgroup with significantly longer PFS and overall survival ($P = 0.013$ and $P = 0.0028$, respectively).

Conclusions: Increased B cells in pre-treatment HNSCC biopsy samples correlate with prolonged benefit from PD-1-based immunotherapy and could further enhance the predictive value of PD-L1 expression.

Key words: B lymphocytes, programmed cell death 1 receptor, head and neck neoplasms, immunotherapy, lymphocytes, tumor infiltrating

INTRODUCTION

Head and neck cancer is estimated to account for over 1 million cases each year globally by the end of this decade, with 467 117 new disease-related deaths reported in 2020.[1] Histologically, head and neck cancer most commonly originates from squamous epithelia and etiologically, it can be grouped into two large categories: tumors linked to infection with high-risk human papillomavirus (HPV) and tumors arising after chronic mutagenesis due to smoking and alcohol, with the former exhibiting more favorable prognosis than the latter.[2] Irrespective of causality, most head and neck squamous cell carcinomas (HNSCCs) will be diagnosed as locally advanced disease. Although at locally advanced disease stage multimodality regimens with surgery, chemotherapy, and irradiation have curative intent, in the case of unresectable recurrent and/or metastatic (R/M) HNSCC, prognosis is dismal even after standard-of-care treatment.[3]

Immune checkpoint inhibitors have been introduced in treatment paradigms of R/M HNSCC and currently

*Correspondence to: Prof. Amanda Psyrri, Department of Internal Medicine, Section of Medical Oncology, Attikon University Hospital, National Kapodistrian University of Athens, Rimini 1, Haidari 12, Athens, Greece. Tel: +30 210 58311265

E-mails: dpsyrri@med.uoa.gr or psyrri237@yahoo.com (A. Psyrri).

constitute the standard of care in the first-line setting either alone or in combination with chemotherapy.[4,5] However, in contrast with the success of immune checkpoint inhibition (ICI) in other solid tumors, such as melanoma, response rate in patients with HNSCC has been confined to a small (13%-18%) population of patients.[4-7] Programmed death-ligand 1 (PD-L1) expression has shown a positive correlation with immunotherapy efficacy[4,5,7] and its assessment by immunohistochemistry and quantification as combined proportion score (CPS) is now part of routine clinical evaluation. CPS corresponds to both PD-L1-positive cancer and stromal immune cells and is the only clinically approved biomarker for patient selection for PD-1 therapy of HNSCC.[8] Nonetheless, biomarker analysis in multiple clinical trials has identified a percentage of patients who experience benefit from ICI regardless of PD-L1 positivity.[9-12] The relatively low frequency of responders among PD-L1-high patients indicates the implication of additional tumor- and host-specific factors in defining immunotherapy outcomes.

The mechanism of action, and hence the success of ICI, relies on a well-orchestrated, highly functional immune network, and its recruitment toward tumor elimination. Consequently, various factors within the tumor immune microenvironment (TIME) have been proposed and investigated as candidate immunotherapy biomarkers in HNSCC.[13] Increased T-lymphocytic infiltration has been described as a positive prognostic characteristic, associated with improved immunotherapy outcomes in HNSCC,[14,15] and in combination with other molecular and cellular markers of immune activation, characterizes a prognostically favorable, 'immune inflamed' tumor phenotype.[16] The role of B cells in immunotherapy response is less investigated.

Here, we evaluated tumor infiltration by diverse immune cell phenotypes including cytotoxic and regulatory T-cell populations as well as B-cell populations, in pre- and post-immunotherapy tissue samples from R/M HNSCC patients.

PATIENTS AND METHODS

Study design and cohort characteristics

Our study population consisted of 60 patients with primary HNSCC, enrolled in the observational biomarker study NCT#03652142, conducted at Attikon University Hospital, National Kapodistrian University of Athens, between 2017 and 2019. Tissue biopsies and peripheral blood samples were prospectively obtained from each patient at baseline and, after safety and accessibility assessment, at two additional timepoints: after two cycles of nivolumab (240 mg administered intravenously every 2 weeks) and at disease progression (Supplementary Figure S1, available at https://doi.org/10.1016/j.annonc.2023.12.011). Follow-up by imaging was carried out every 3 months during treatment and cases were annotated for best overall response to immunotherapy, assessed using RECIST, version 1.1, as complete response (CR), partial response (PR), stable disease (SD), or progressive disease (PD). Epidemiologic and relevant clinical information, as well as progression-free survival (PFS) and overall survival (OS) were also calculated based on database as of 1 August 2021 (Table 1). Disease control was defined as either CR or PR or SD versus PD. Written informed consent was provided by all patients. The study was approved by the ethics committee/institutional review board of Attikon University Hospital, Haidari, Athens, Greece (protocol # ΒΠΠΚ, ΕΒΔ2840/21-11-2017) and conducted in accordance with the Declaration of Helsinki.

Table 1. Clinicopathological characteristics

	Patient cohort, *n* (%)
Age (years)	
Median (min, max)	64.0 (40.1, 90.9)
Sex	
Male	49 (82)
Female	11 (18)
R/M status	
Recurrent	43 (72)
Metastatic	17 (28)
Smoking (current/former)	
Yes	42 (70)
No	10 (17)
Unknown	8 (13)
Alcohol (current/former)	
Yes	21 (35)
No	28 (47)
Unknown	11 (18)
HPV status	
Positive (oropharynx)	4 (7)
Negative (oropharynx)	11 (18)
Unknown (oropharynx)	0 (0)
Positive (other sites)	0 (0)
Negative (other sites)	2 (3)
Unknown (other sites)	43 (72)
Primary site	
Oral cavity	24 (40)
Larynx	19 (32)
Oropharynx	15 (25)
Other	2 (3)
Best overall response	
Complete response	2 (3.3)
Partial response	6 (10.0)
Stable disease	10 (16.7)
Progressive disease	42 (70.0)
Progression-free survival (months)	
Mean (SD)	7.20 (9.95)
Overall survival (months)	
Mean (SD)	11.8 (9.66)

HPV, human papillomavirus; R/M, recurrent and/or metastatic; SD, standard deviation.

Multispectral imaging and data analysis

Multiplex immunofluorescence (IF) images were acquired on Vectra 3.0 automated quantitative pathology imaging system (Akoya Biosciences, Marlborough, MA). Tissue- and panel-specific spectral library of each individual fluorophore in the panel and tumor tissue autofluorescence were acquired for an optimal IF signal unmixing (individual spectral peaks) and multiplex analysis. IF-stained slides were prescanned at ×10 magnification. Using the Phenochart™ whole-slide viewer (Akoya Biosciences), up to 20 regions of interest containing tumor islets and stroma were annotated by a pathologist for high-resolution multispectral

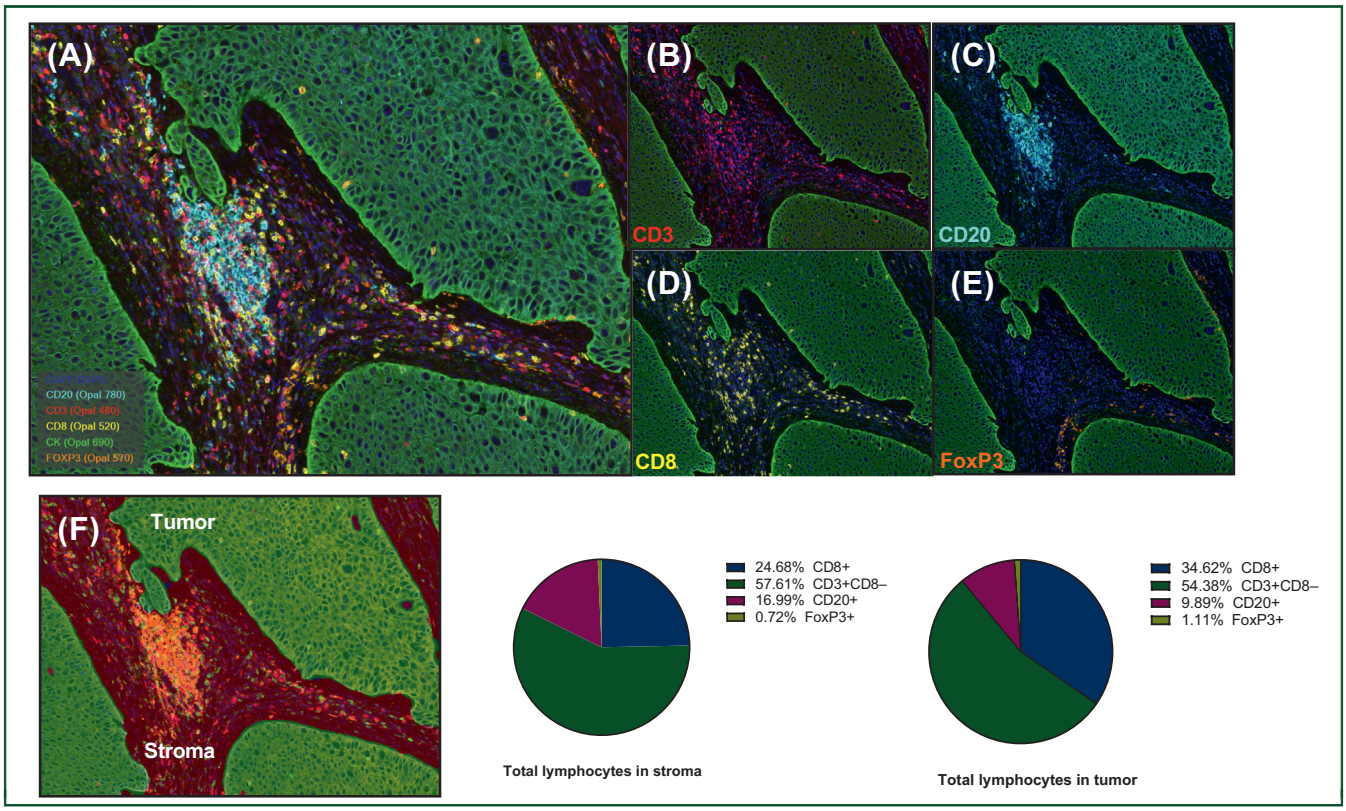

Figure 1. Multiplex immunofluorescence staining; representative region of interest containing a tertiary lymphoid structure. (A) Composite image. (B-E) Immune phenotypes. (F) Tissue segmentation in tumor (green) and stroma (red) and % of immune phenotypes in each segment.

acquisition of images at ×20 magnification. IF signal extractions were carried out using inForm 2.3.0 image analysis software (Akoya Biosciences, Marlborough, MA) enabling a per-cell analysis of IF markers of multiplex stained tissue sections. The images were first segmented into tumor and stroma regions, based on the cytokeratin staining using the inForm Tissue Finder™ algorithms. Individual cells were then segmented using the counterstain-based cell segmentation algorithm, based on DAPI staining. Quantification of the immune cells was carried out using the inForm scoring tool by assigning a threshold to the different cell phenotypes across several images, based on the staining intensity of each marker. IF-stained cohorts are then batch processed, and data were exported and processed via an in-house developed R script algorithm (Post-inForm) to retrieve every cell subpopulation (Figure 1).

RNA in situ hybridization spatial transcriptomics

Messenger RNA (mRNA) *in situ* gene expression data obtained from tumor microarray YTMA496 (GSE226134), which comprised the same cases as the NCT#03652142 study, were analyzed to provide an orthogonal validation of our findings. As described in previous publications,[17,18] high-plex spatial detection of mRNA *in situ* was carried out according to the NanoString GeoMx RNA assay protocol (MAN-10087-03) using the Whole Transcriptome Atlas probe reagent, for three molecularly defined tissue compartments: tumor (PanCK), leukocyte (CD45), and macrophage (CD68). Library preparation consisted of one library per compartment and sequencing was carried out using the Illumina NovaSeq platform. Raw sequencing reads were obtained after combining the Illumina sequencing FASTQ files and the NanoString (Seattle, WA) GeoMx DSP configuration files, and digital count conversion files were created and uploaded into the GeoMx DSP Instrument. The final gene expression counts were obtained following quality control (QC) and Q3 normalization.

For the purposes of the present study, gene set enrichment analysis (GSEA) was carried out in the tumor and leukocyte compartments utilizing previously described methodology,[19] for groups of genes associated with B cells and tertiary lymphoid structures (TLSs) obtained from the literature[20,21] (Supplementary Table S1, available at https://doi.org/10.1016/j.annonc.2023.12.011).

Immunohistochemical/IF staining and flow cytometry methods, as well as TLS evaluation and immune phenotype assessment are detailed in Supplementary Materials and Figure S2, available at https://doi.org/10.1016/j.annonc.2023.12.011.

Statistical analysis

According to the study design, a minimum of 50 cases was required to reach statistical power of 80%. The number of required cases was increased to 60 during the study (amendment is pending), due to many biopsy samples failing to pass QC. Pearson's correlation coefficient (R) was used to examine the linear association between different immune cell phenotypes. Comparison of non-continuous

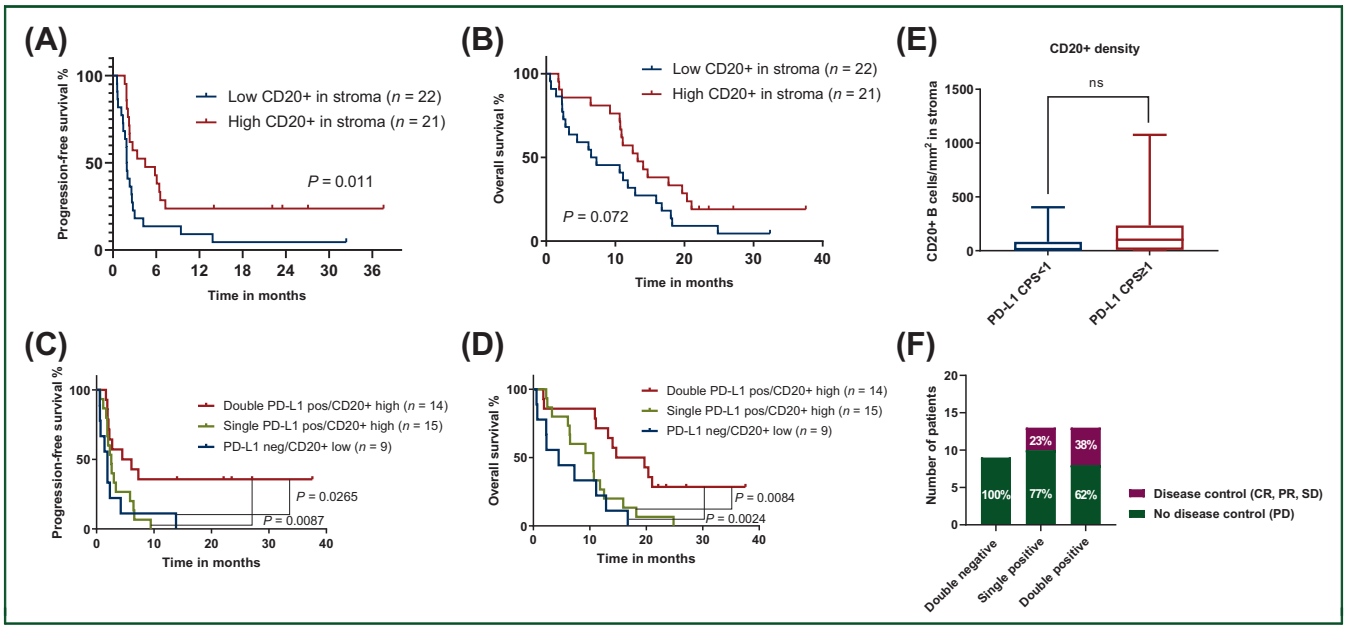

Figure 2. B-cell density shows predictive value for IO in HNSCC and improves PD-L1-based patient stratification. (A, B) Increased CD20+ B-cell density correlates with improved PFS and shows a trend for longer OS. (C, D) Increased CD20+ B-cell density is associated with improved PFS and OS in PD-L1-positive tumors. (E) B-cell density contributes to improved survival outcomes independently of PD-L1 expression. (F) Single-positive and double-positive subgroups are enriched with patients experiencing disease control.

CPS, combined proportion score; CR, complete response; HNSCC, head and neck squamous cell cancer; IO, immunotherapy; OS, overall survival; PD, progressive disease; PD-L1, programmed death-ligand 1; PFS, progression-free survival; PR, partial response; SD, stable disease.

variables was carried out using the Mann–Whitney *U* test for two groups and the Kruskal–Wallis H test for three or more groups. Survival curves for OS and PFS were constructed using the Kaplan–Meier estimator and statistical significance was determined using the log-rank test. Multivariate analysis was carried out using the Cox proportional hazards model. Correction for multiple testing was carried out using the Benjamini–Hochberg method (false discovery rate 0.05). Cases were stratified into high and low infiltrated groups by using the median as a cut-off for CD20+ B cells and the rest of immune cell populations based on previous publications.[22-24] PD-L1 CPS 1 was the cut-off used to stratify positive (CPS $\geq$ 1) and negative (CPS $<$ 1) PD-L1 cases. For the GSEA, differential gene expression analysis was carried out for each tissue compartment and genes were ranked based on their log (fold-change) for the outcomes of response and disease control. Then ranked genes were analyzed using the GSEApy package[19] to obtain the gene set enrichment results. Hypothesis testing was carried out at a two-sided significance level of $\alpha = 0.05$. Statistical analyses were carried out using GraphPad Prism v9.0.2 software (GraphPad Software, La Jolla, CA, RRID:SCR_002798) and RStudio 1.4.1106 (RStudio, PBC, Boston, MA).

RESULTS

CD20+ B-cell stromal density is associated with improved PFS

Univariate OS and PFS analyses were carried out on pretreatment immune cell densities, both in tumor and stromal compartments, using CD8+, CD3+/CD8−, FoxP3+, and CD20+ markers for cytotoxic, CD4+ T helper cells, regulatory T cells (Tregs), and B lymphocytes, respectively. Forty-five out of total 60 baseline biopsies passed QC after pathologist assessment and clinicopathological characteristics were similar between analyzed and excluded cases. Out of 45 baseline biopsies that underwent IF staining, 1 case was excluded from the analysis due to poor tissue quality, and 1 was ineligible for CD20+ quantification due to high autofluorescence. CD20+ B-cell density in the stromal but not in the tumor tissue compartment was associated with prolonged PFS [hazard ratio (HR) 0.44, 95% confidence interval (CI) 0.23-0.84, $P = 0.011$] (Figure 2A and B), while none of the other immune cell populations either in tumor or in stroma were found to significantly affect survival

Table 2. Association of baseline immune cell density (cells/mm²) with PFS for each tissue compartment and lymphocytic phenotype

Tissue compartment	Immune cell phenotype (median)	Log-rank *P* value	Univariate HR (95% CI)	Multivariate *P* value
Stroma	CD8+	0.84	0.93 (0.49-1.78)	
	CD3+/CD8−	0.83	1.07 (0.56-2.05)	
	FoxP3+	>0.9	0.98 (0.51-1.86)	
	CD20+	**0.011**	0.44 (0.23-0.84)	**0.026**
Tumor	CD8+	0.83	0.93 (0.49-1.78)	
	CD3+/CD8−	0.786	0.91 (0.48-1.74)	
	FoxP3+	>0.9	0.98 (0.51-1.86)	
	CD20+	0.244	0.2 (0.36-1.30)	

B-cell density in stroma is significantly associated with improved PFS and maintains its significance in a multivariate model. CD20+ cell density in stroma showed association with PFS both in univariate and multivariate analyses (*P* values in bold).
CI, confidence interval; HR, hazard ratio; PFS, progression-free survival.

https://doi.org/10.1016/j.annonc.2023.12.011

(Table 2). A similar trend was observed for CD20+ B cells in association with OS without reaching statistical significance (Supplementary Table S2, available at https://doi.org/10.1016/j.annonc.2023.12.011). The PFS association was also maintained in the multivariate analysis, after adjusting for relevant clinical prognostic factors (Supplementary Figure S3, available at https://doi.org/10.1016/j.annonc.2023.12.011). B-cell stromal density also showed a positive correlation with other immune subpopulations, predominantly with CD3+/CD8− T cells that largely consist of CD4+ T cells, and with CD8+ T cells and FoxP3+ T cells (Supplementary Figure S4A-C, available at https://doi.org/10.1016/j.annonc.2023.12.011).

In pre-treatment biopsy specimens, high plasma cell (PC) infiltration, defined as the presence of common small aggregates or large PC aggregates/sheets on hematoxylin–eosin, was also associated with prolonged PFS (HR 0.38, 95% CI 0.2-0.72, $P = 0.0079$) and had a similar trend for OS (Supplementary Figure S5A and B, available at https://doi.org/10.1016/j.annonc.2023.12.011). Cases rich in PCs correlated with increased stromal CD20+ B-cell density compared with PC-low tumors. Still, they showed no correlation with other immune cell populations (Supplementary Figure S5C, available at https://doi.org/10.1016/j.annonc.2023.12.011) and while most CD20-low samples comprised PC-low cases, CD20-high samples were more evenly distributed between PC categories (Supplementary Figure S5D, available at https://doi.org/10.1016/j.annonc.2023.12.011). These findings underscore the essential role of terminal B-cell differentiation into antibody-producing PCs in enhancing the therapeutic efficacy of nivolumab.

CD20+ B-cell stromal density improves PD-L1-based patient selection for ICI treatment in HNSCC

The impact of stromal CD20+ B-cell densities on survival prompted us to investigate a potential refinement of the PD-L1 expression status as a predictor of outcomes. To replicate currently clinically applied practices, CPS 1 was used to divide our cohort into PD-L1-positive (CPS $\geq$ 1) and PD-L1-negative cases (CPS $<$ 1). Regarding CD20+ B-cell stromal density, cases were, once again, separated by the median.

In concordance with the biomarker analysis of the KEYNOTE 048 study,[5] PD-L1 positivity in our study was also associated with increased OS (HR 0.33, 95% CI 0.15-0.73, $P < 0.001$) in univariate and multivariate analyses. PD-L1 status did not correlate with PFS (Supplementary Figure S6A-C, available at https://doi.org/10.1016/j.annonc.2023.12.011). We therefore tested if the combination of PD-L1 and stromal CD20 markers would better stratify patients. PD-L1/CD20 double-positive patients demonstrated a significant survival advantage compared to double-negative tumors both for PFS (median PFS 5.3 months versus 1.9 months, HR 0.31, 95% CI 0.11-0.93, $P = 0.0087$) and for OS (median OS 17.2 months versus 4.5 months, HR 0.28, 95% CI 0.1-0.88, $P = 0.0024$). Furthermore, patients with either PD-L1−/CD20+ or with PD-L1+/CD20− phenotypes also demonstrated decreased PFS and OS (median PFS 5.3 months versus 2.6 months, HR 0.41, 95% CI 0.18-0.93, $P = 0.0265$ and median OS 17.2 months versus 10.6 months, HR 0.37, 95% CI 0.16-0.83, $P = 0.0084$, respectively) compared with PD-L1/CD20 double-positive cases (Figure 2C and D). Notably, B-cell levels in stroma showed no overlap with either PD-L1-positive or PD-L1-negative cases, suggesting that each factor exerts its effect independently (Figure 2E). Of note, PD-L1 positivity was also not associated with any of the remaining quantified immune cell phenotypes (Supplementary Figure S6D, available at https://doi.org/10.1016/j.annonc.2023.12.011). Finally, there is a clear enrichment in the double PD-L1+/CD20+ high category with cases experiencing disease control (CR, PR, SD) (38%), in comparison with single-positive or double-negative classes (23% and 0%, respectively) (Figure 2E). Combined, the above findings illustrate that B-cell density adds to the predictive value of PD-L1 and identifies the subgroup of patients among PD-L1 expressors, with the highest likelihood to benefit from immunotherapy.

Subsequently, we hypothesized that high B-cell density in stroma is associated with the formation of TLS. As expected, there was a clear association of the presence/absence of TLS and CD20+ B cells in stroma (Supplementary Figure S6E, available at https://doi.org/10.1016/j.annonc.2023.12.011) but only half of CD20+ high cases (as were previously defined dichotomized by the median) also harbored at least one TLS (Supplementary Figure S6F, available at https://doi.org/10.1016/j.annonc.2023.12.011). Notably, survival analysis was carried out between the 38 TLS-negative cases and the 12 TLS-positive cases and TLS presence was not significantly associated with either PFS or OS (Supplementary Figure S6G and H, available at https://doi.org/10.1016/j.annonc.2023.12.011).

B-cell gene enrichment in stroma correlates with response and disease control

To validate our findings, we carried out GSEA in available mRNA *in situ* expression data from patients of our study cohort (GSE226134), for B-cell- and TLS-associated genes. The CD45 pan-leukocyte marker was used as a surrogate to define the stroma compartment. Stromal enrichment with B-cell-associated genes showed association with both response ($P = 0.027$) and disease control ($P = 0.038$) to nivolumab, as opposed to tumor-infiltrating leukocyte (TIL)-associated genes; neither germinal center-specific (indicating mature TLS) nor other known TLS-related gene expression in stroma showed association with response or disease control (Figure 3A, Supplementary Figure S7A, available at https://doi.org/10.1016/j.annonc.2023.12.011). Conversely, in the tumor compartment, B-cell gene enrichment had no association with response or disease control. However, TLS-related gene expression in tumor correlated with disease control, possibly indicating an overall 'immune inflamed' phenotype for these cases (Figure 3B,

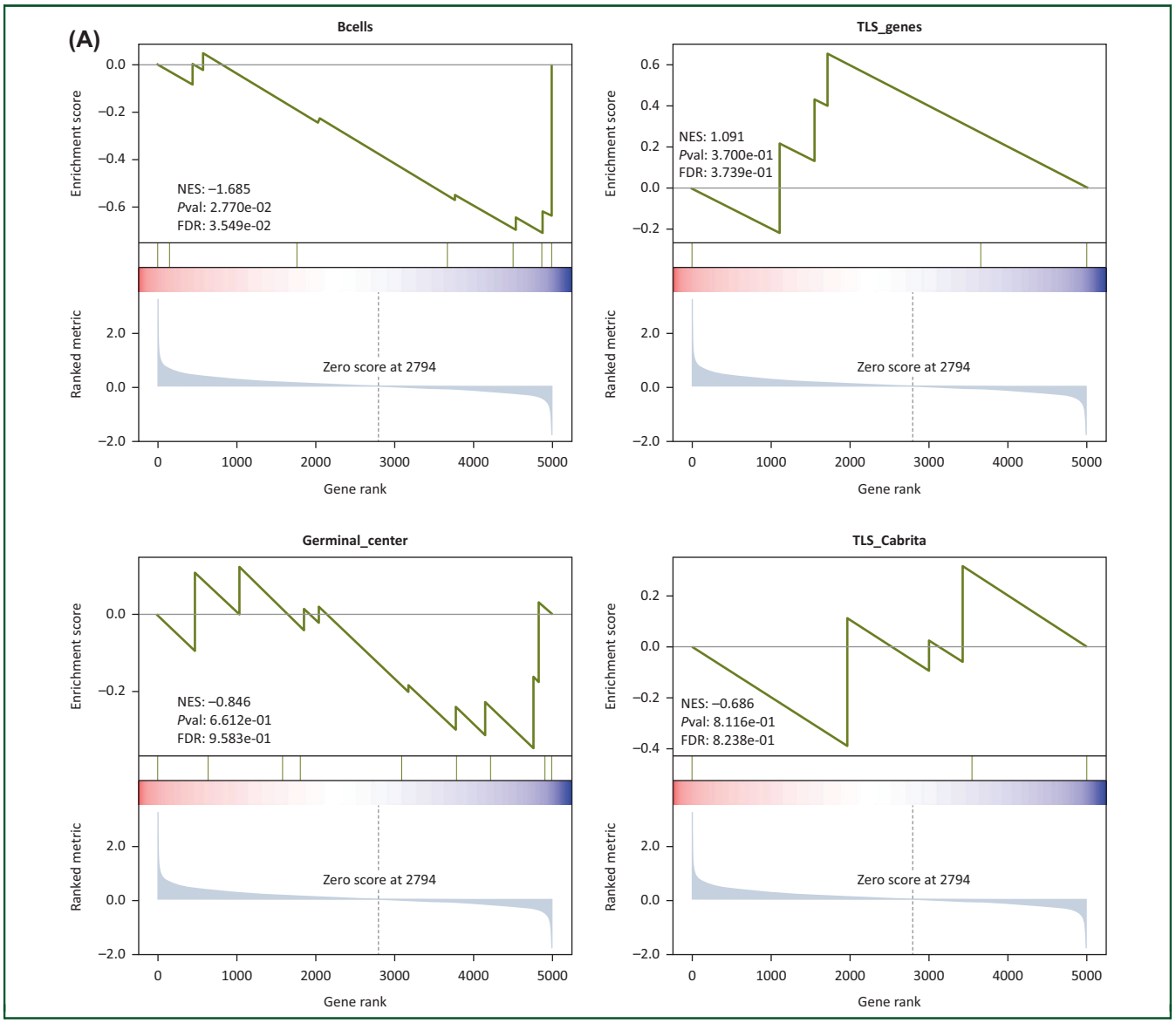

Figure 3. Gene set enrichment analysis for genes associated with B cells and tertiary lymphoid structures (TLSs). (A) Stromal enrichment with B-cell-related genes is associated with response to immunotherapy, while TLS-related gene sets show no association with response. (B) Neither B-cell- nor TLS-related gene enrichment in the tumor compartment shows association with response.
FDR, false discovery rate; NES, normalized enrichment score.

Supplementary Figure S7B, available at https://doi.org/10.1016/j.annonc.2023.12.011).

Immunotherapy transforms TIME toward the 'immune inflamed' phenotype

Next, we sought to identify potential immunotherapy-induced alterations in the morphology and composition of HNSCC TIME. In total, 30 pairs of matched biopsies obtained at two separate timepoints, (i) pre-immunotherapy and (ii) after two cycles of treatment, were available for analysis after quantitative IF with the same panel.

Again, we defined the three major cancer inflammation types. After two cycles of immunotherapy, 'immune inflamed' cases increased by 29%, while the number of 'immune excluded' and 'immune desert' cases was reduced by 2% and 27%, respectively. In a subset of patients, 'immune excluded' and 'immune desert' cases, i.e. 'cold tumors', as have been characterized in previous immune cell quantification-based studies,[25-27] were found to switch category to 'immune inflamed' tumors (Figure 4A and B). Subsequently, we hypothesized that the identified post-treatment switch might be linked to improved response to immunotherapy. While patients with an 'inflamed' immune profile at baseline exhibited better disease control, a similar association was not identified in post-treatment cases (Supplementary Figure S8A and B, available at https://doi.org/10.1016/j.annonc.2023.12.011). This might indicate that the initial state of inflammation is critical to define responsiveness, whereas the acquisition of inflamed states during immune therapy has no

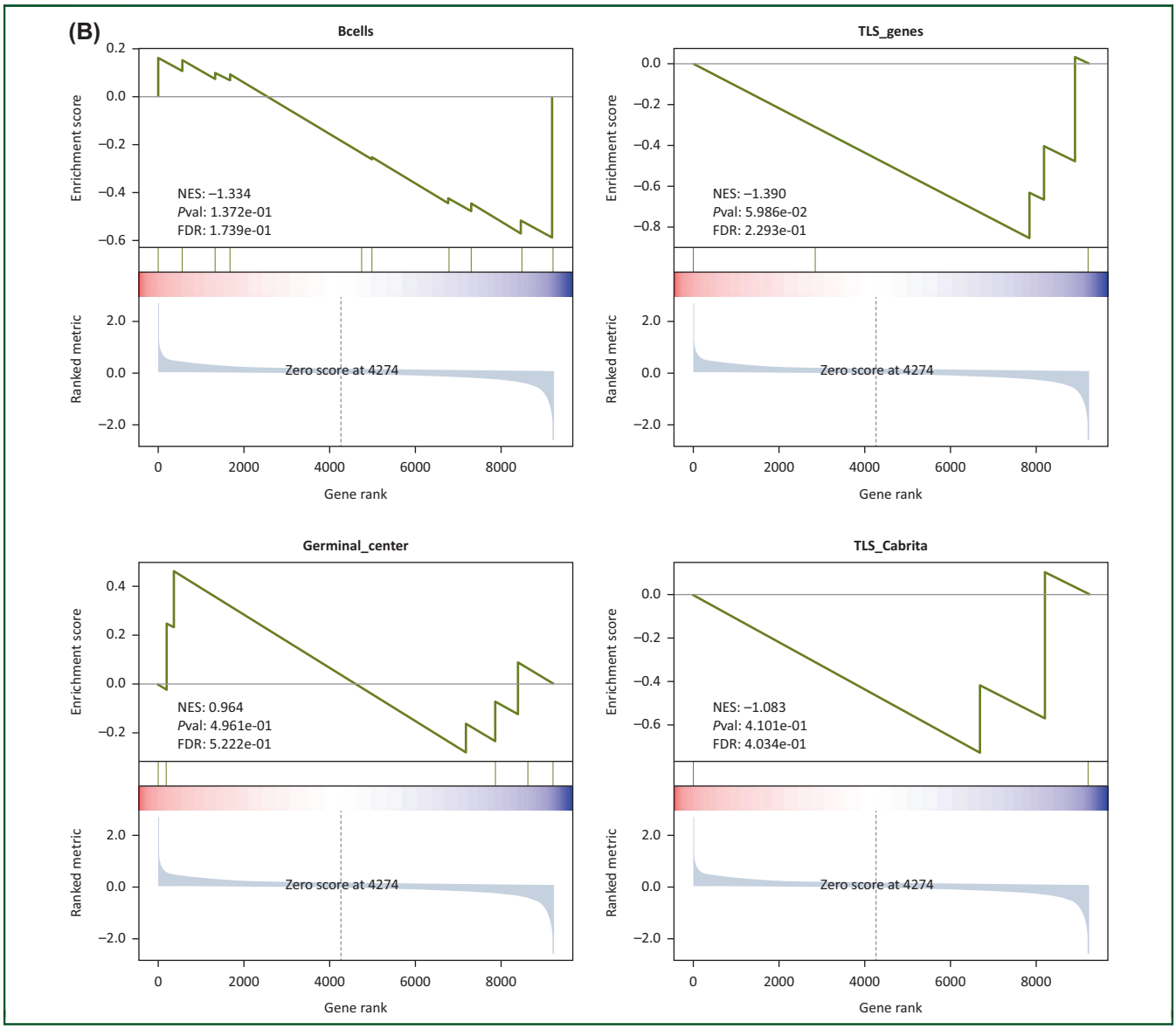

Figure 3. Continued.

impact on the efficacy of ICIs. It should be noted that due to the relatively small number of evaluable post-treatment biopsies, the study was underpowered to detect a potential correlation between phenotypic switch and response.

We also examined the potential pre- and post-immunotherapy fluctuation in the percentage of immune cells (among total cells) of the tumor and stromal compartments. In the stromal compartment, none of the immune subpopulations demonstrated a significant percentage alteration (Figure 4C). Conversely, in the tumor compartment, the percentage of CD3+, CD8+, and CD3+/CD8− immune cells was significantly increased post-treatment, suggesting an enhanced intratumoral T-lymphocytic infiltration (Figure 4D). No significant change in the frequency of CD20+ B cells and FoxP3+ Tregs was observed, either in tumor or stroma, and PD-L1 expression was not associated with any of the three immune phenotypes (Supplementary Figure S8C, available at https://doi.org/10.1016/j.annonc.2023.12.011). Finally, matched biopsy samples were also available at disease progression for nine cases. A significant decrease in CD3+/CD8− cells in tumor was observed between the on-treatment and disease progression timepoints; however, a bigger sample size is needed before drawing definite conclusions (Supplementary Figure S9A and B, available at https://doi.org/10.1016/j.annonc.2023.12.011).

Flow cytometric analysis of pre-treatment peripheral blood mononuclear cells identifies immune cell phenotypes associated with response to ICIs

Ultimately, we hypothesized that the identification of specific tumor immune characteristics, with differential association with immunotherapy outcomes, might simultaneously correspond to a distinct immune cell profile in the periphery. To this end, we carried out flow cytometric analysis on pre-treatment peripheral blood mononuclear

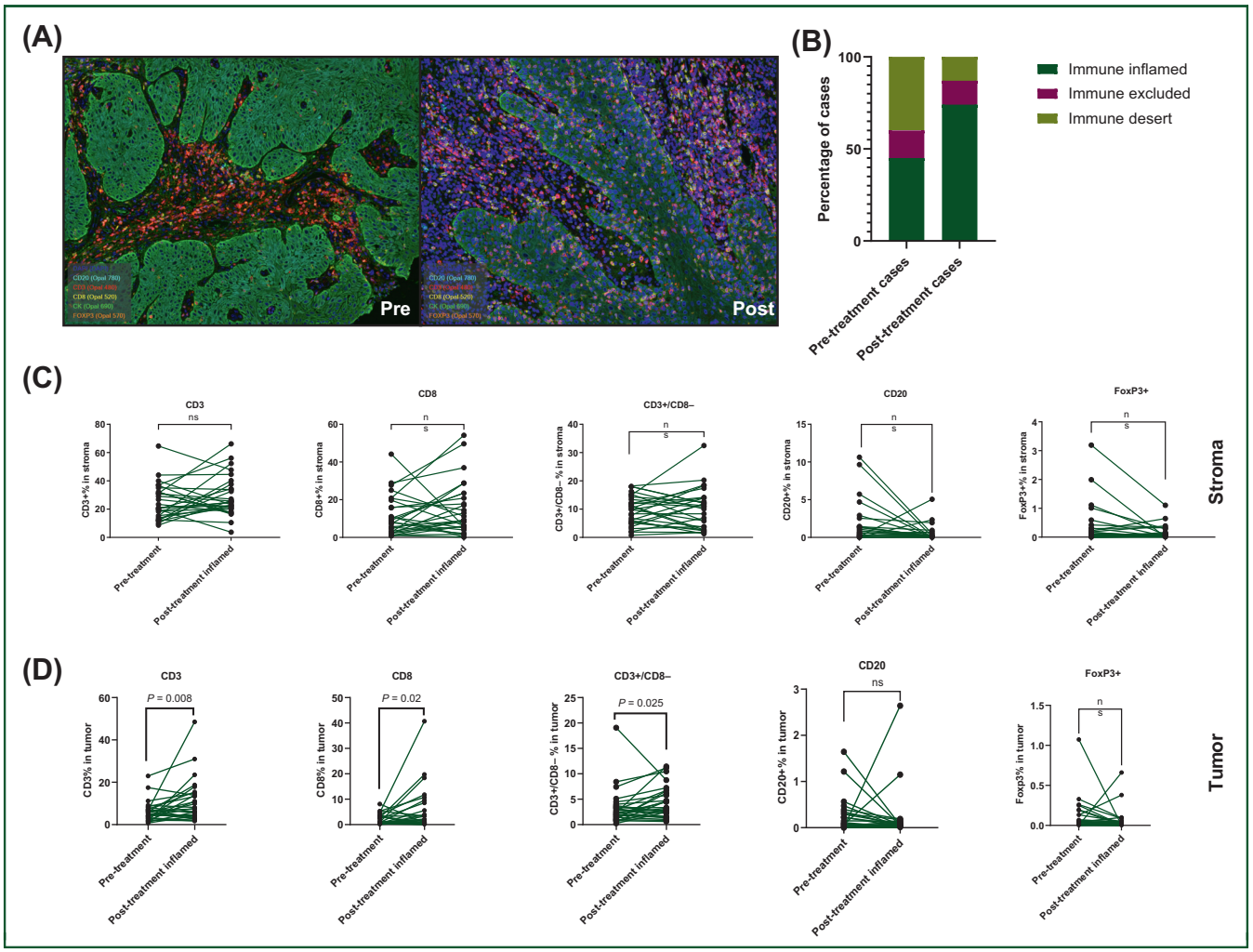

Figure 4. Observed alterations in immune cell spatial distribution and phenotypic composition post-immunotherapy treatment. (A) Representative immunofluorescence (IF) images of a pre-treatment 'immune excluded' case, turned 'immune inflamed' post-treatment. (B) 'Immune inflamed' tumor microenvironment (TME) phenotype frequency is favored post-immunotherapy. Immune cell percentage (of total cells for each compartment) variations post-immunotherapy in stroma (C) and tumor (D). While immune cell percentages show no alteration in stroma, intratumoral total T-lymphocyte as well as CD8+ and CD4+ T-cell percentage is significantly increased post-treatment.

cells. Correlation of immune cell sub-phenotypes with response to immunotherapy led to the identification of a distinct cell cluster among responders, primarily consisting of increased populations of proliferating (Ki67+) CD8+ and CD4+ T cells with stem-like (TCF-1+) or exhaustion (TOX+) characteristics. Additionally, baseline CD21−/low B cells, a previously characterized memory cell phenotype, exhibited increased levels in the responders' subgroup (Supplementary Figure S10, available at https://doi.org/10.1016/j.annonc.2023.12.011). These findings are in line with previous reports, suggesting the preferentially improved effectiveness of ICIs in the presence of 'progenitor exhausted' (TCF-1+/PD-1+) T-cell populations.[28] Additionally, increased percentage of unswitched memory [immunoglobulin D (IgD)/IgM+] B cells was significantly associated with the absence of clinical benefit. Conversely, higher levels of peripheral plasmablast (CD38++IgM−) % B cells at baseline were observed in patients experiencing clinical benefit. This might indicate that distinct memory cell phenotypes differentially affect treatment outcomes. Associations of the rest of pre-treatment immune cell sub-phenotypes with clinical benefit, disease control, and response are summarized in Supplementary Tables S3-S5, available at https://doi.org/10.1016/j.annonc.2023.12.011.

DISCUSSION

In this study, we sought to investigate possible associations of immune cell populations with immunotherapy outcomes and specify their spatiotemporal alterations following ICI within the HNSCC TIME. Nivolumab is approved in the United States and Europe in platinum-refractory R/M HNSCC regardless of PD-L1 expression. Pembrolizumab alone or with chemotherapy is approved in Europe in patients with CPS $\geq$1 in the first-line R/M setting. The objective response rate to single-agent pembrolizumab is around 19% in PD-L1-positive (CPS $\geq$ 1) R/M HNSCC population,[5]

indicating that the majority of PD-L1 expressors exhibit resistance to ICI.

Here, we have shown that increased stromal B-cell density in pre-treatment biopsy samples of R/M HNSCC improves patient selection for single-agent immunotherapy, as it characterizes a subgroup of PD-L1 expressors with improved survival outcomes after anti-PD-1 treatment. On the contrary, immunotherapy delivers worse results among PD-L1 expressors with concomitantly low CD20+ B-cell infiltration, a patient subgroup for which more intensified treatment paradigms, such as the combination of immunotherapy with chemotherapy or other targeted agents, might prove beneficial.

In the present study, none of the other immune cell populations (i.e. CD8+, CD4+, FoxP3+) that were investigated showed association with either OS or PFS. Several studies on the prognostic effect of TILs in HNSCC have reported conflicting results.[29-32] However, it should be noted that these studies included cases of various anatomical subtypes, stages, and treatments and TIL assessment was carried out by different cut-offs and assays in total tissue area rather than in tumor and stroma.

While the prognostic effect of tumor-infiltrating T cells in HNSCC—mainly CD8+ cytotoxic and CD4+ T helper cells—has been rigorously investigated,[14,33,34] the precise dynamic of B cells in antitumor immune interactions has yet to become clearly elucidated. Several studies suggest that B cells are tumor-promoting, while others demonstrate a positive association with improved cancer outcomes, particularly when they are found in association with TLSs. In a systematic review of the literature, B-cell and PC infiltration was found to have a positive prognostic impact in several solid tumor studies including non-small-cell lung cancer (NSCLC), breast cancer, colorectal carcinoma, ovarian cancer, and melanoma.[35] The uncertainty about the immune-enhancing or immunosuppressive nature of B cells is partially attributed to opposing functions elicited by diverse B-cell phenotypes, production of cancer antigen-specific antibodies toward antibody-dependent cellular cytotoxicity (ADCC), T-cell priming by antigen presentation, and maintenance of durable immune responses through participation in TLSs, which constitute tumor-eliminating B-cell qualities. In contrast, a subgroup of tumor-infiltrating B cells with regulatory characteristics has been described to drive tumor immune escape through the secretion of immunosuppressive cytokines, the up-regulation of immune checkpoint molecules, and the inhibition of T-cell proliferation and activity.[36]

In recent years, several seminal reports have illustrated the positive predictive effect of B cells—either alone or as part of TLS—on cancer immunotherapy in melanoma and soft-tissue sarcoma cohorts.[20,37,38] Gene expression analysis in NSCLC patients treated with ICI has also revealed the association of both B-cell and total TIL gene signatures with improved PFS and response, as opposed to PD-L1 mRNA expression.[21] Accordingly, in a multi-tumor array study, the presence of a 'mature' TLS subset, characterized by CD23+ follicular T-cell presence, was also associated with increased immunotherapy response rate and PFS.[39] In the same study, only 5 out of 12 HNSCC cases were TLS positive. Similarly, in the present study, there were only 12 TLS-positive cases; thus we were underpowered to carry out further analysis based on TLS maturation status using the CD21 and CD23 markers as has been previously proposed.[40] TLS presence has also been identified as a favorable prognostic factor in HNSCC.[41] It has been postulated that the substantial heterogeneity in the cellular constituents of TLSs and their location within tumors may influence the overall effect on antitumor immunity and outcome.[42-45] Here, we demonstrate that B-cell density and B-cell gene enrichment in stroma are correlated with improved immunotherapy outcomes in HNSCC, independently of the formation of TLS; however, TLS assessment was done regardless of maturation status.

In HNSCC, analysis of The Cancer Genome Atlas RNA sequencing data has also illustrated a potentially prognostic effect of B cells, as CD19 expression was positively correlated with OS and 3-year survival rate, especially in the highly immunogenic subgroup of HPV+ HNSCC. In concordance with our results, in the same study, B-cell depletion in murine HPV+ HNSCC models treated with an anti-PD-L1 agent, or radiation therapy or the combination of both, led to increased tumor proliferation, indicating that B-cell presence is tightly linked to the efficacy of immune checkpoint blockade. In the present study, CD20+ B-cell density, specifically in the stromal compartment, correlated with improved PFS and disease control in a cohort treated exclusively with anti-PD-1 monotherapy. The effect of stromal B-cell density on PFS and, most importantly, the enhancement of the predictive value of PD-L1 expression after combining the two factors clearly indicate the specific association of infiltrating B cells with immunotherapy outcomes. This effect potentially relies on antibody secretion and ADCC, as was suggested by the correlation of PC presence with B-cell density and the association of PCs with PFS. Previous reports have shown that tumor-infiltrating B cells and PCs participate in the production of HPV antigen-specific antibodies.[46] Increased
B-cell infiltration and their localization within germinal center-resembling areas within TLS have been correlated with prolonged OS,[47] whereas decreased expression of genomic PC markers has been associated with poor disease-specific survival in HPV+ HNSCC.[48]

To our knowledge, this is the first study to provide insight into R/M HNSCC TIME transformation under the influence of ICI, using repeated on-treatment biopsies. We used a well-described TIME classification based on cell quantification among tissue to stratify cases into three categories: 'immune inflamed', 'immune excluded', and 'immune desert'. A similar classification has been also proposed using bulk RNA deconvolution in melanoma[49]; however, it should be noted that bulk RNA deconvolution tools could not be applied here, as the GSE226134 dataset comprises only spatial RNA data. Interestingly, repeated tumor biopsies

obtained following two cycles of ICI showed increased overall intratumoral immune cell infiltration and the 'immune inflamed' phenotype was acquired by an additional 30% of cases in comparison with pre-treatment samples. CD8+ and CD4+ T cells were the two subsets that showed significant intratumoral increase in post-immunotherapy tissue samples. This shift is consistent with results from a pilot study investigating the effect of intralesional injection of pembrolizumab in high-risk ductal carcinoma *in situ*, where post-immunotherapy CD8+ and CD4+ T-cell populations increased in contrast with other immune cell subtypes, including B cells and Tregs.[50]

The therapeutic rationale for PD-1/PD-L1 axis inhibition is to reinstate antitumor activity of previously suppressed T cells and thus stimulate host immunity toward cancer elimination. In this study, the increase in immune cell percentage was predominantly observed in the tumor compartment, indicating that ICI not only re-establishes T-cell activation but also stimulates, possibly chemotactically, T-cell recruitment in the tumor bed. The post-immunotherapy expansion of immune cell infiltration has been previously linked to improved clinical activity, in a study exploring the effect of anti-cytotoxic T-lymphocyte-associated protein 4 monoclonal antibody ipilimumab in melanoma TIME.[51] Here, we found no correlation of post-treatment immune status with disease control. In contrast, disease control was achieved primarily in cases with a baseline 'immune inflamed' status, suggesting that immunotherapy response relies on highly functional, pre-existing host immunity. Due to the small number of matched pre- and post-treatment biopsies, however, definite conclusions cannot be drawn.

We would like to acknowledge the relatively small sample size of our cohort as a limitation of our study. The low proportion of HPV-related tumors, mainly due to few oropharyngeal tumors, was also a limitation for further assessment of this population. Additionally, the small number of TLS-positive cases did not allow for analysis based on stratification by TLS maturity. Finally, a limitation of this study was the unavailability of additional independent ICI-treated cohorts of R/M HNSCC patients for external validation of our findings.

In conclusion, in the present study, we demonstrate that stromal B-cell density correlates with PFS in ICI-treated cohort of R/M HNSCC. In addition, stromal enrichment with B-cell-associated genes was noted in the tumors of responders versus non-responders. The correlation of intratumoral PCs with PFS in our study suggests that the B cells possibly amplify antitumor immune responses through antibody production. Together, these data provide insights into the potential role of B cells in the response to ICI treatment in HNSCC, with implications for the development of biomarkers and therapeutic targets.

ACKNOWLEDGEMENTS

The authors would like to thank participating patients and their families. They would also like to thank Christakis Risilia, Maria Kelidou, and the technical staff at the 2nd Department of Pathology, Attikon University Hospital, for their excellent, expert assistance.

FUNDING

This study was sponsored by Bristol Myers Squibb (BMS) (Study CA209-8EN). BMS funding was exclusively used for experiments carried out in Greece and Switzerland (no grant number).

DISCLOSURE

AP has served as an advisor for MSD, Nanobiotics, BMS, Astrazeneca, Merck Serono. She has received institutional research funding from BMS, Merck Serono, Roche, Sanofi. DLR has served as an advisor for Astra Zeneca, Agendia, Amgen, BMS, Cell Signaling Technology, Cepheid, Danaher, Daiichi Sankyo, Genoptix/Novartis, GSK, Konica Minolta, Merck, NanoString, PAIGE.AI, Perkin Elmer, Roche, Sanofi, and Ventana. Amgen, Cepheid, NavigateBP, NextCure, and Konica Minolta fund research in DLR's lab. All other authors have declared no conflicts of interest.

DATA SHARING

Data are available upon reasonable request. The R script used in multispectral image data analysis can be found in GitLab repository and downloaded from: https://gitlab.isb-sib.ch/Vital-IT/postinform/-/archive/master/postinform-master.zip. The mRNA *in situ* data generated in this study have been deposited in NCBI's Gene Expression Omnibus and are accessible through GEO Series accession number GSE226134.

REFERENCES

1. Sung H, Ferlay J, Siegel RL, et al. Global cancer statistics 2020: GLOBOCAN estimates of incidence and mortality worldwide for 36 cancers in 185 countries. *CA Cancer J Clin*. 2021;71:209-249.
2. Johnson DE, Burtness B, Leemans CR, Lui VWY, Bauman JE, Grandis JR. Head and neck squamous cell carcinoma. *Nat Rev Dis Pri*. 2020;6:92.
3. Vermorken JB, Specenier P. Optimal treatment for recurrent/metastatic head and neck cancer. *Ann Oncol*. 2010;21:vii252-vii261.
4. Ferris RL, Blumenschein G Jr, Fayette J, et al. Nivolumab for recurrent squamous-cell carcinoma of the head and neck. *N Engl J Med*. 2016;375:1856-1867.
5. Burtness B, Harrington KJ, Greil R, et al. Pembrolizumab alone or with chemotherapy versus cetuximab with chemotherapy for recurrent or metastatic squamous cell carcinoma of the head and neck (KEYNOTE-048): a randomised, open-label, phase 3 study. *Lancet*. 2019;394:1915-1928.
6. Borel C, Jung AC, Burgy M. Immunotherapy breakthroughs in the treatment of recurrent or metastatic head and neck squamous cell carcinoma. *Cancers*. 2020;12:2691.
7. Seiwert TY, Burtness B, Mehra R, et al. Safety and clinical activity of pembrolizumab for treatment of recurrent or metastatic squamous cell carcinoma of the head and neck (KEYNOTE-012): an open-label, multicentre, phase 1b trial. *Lancet Oncol*. 2016;17:956-965.
8. Emancipator K, Huang L, Aurora-Garg D, et al. Comparing programmed death ligand 1 scores for predicting pembrolizumab efficacy in head and neck cancer. *Mod Pathol*. 2021;34:532-541.

9. Bauml J, Seiwert TY, Pfister DG, et al. Pembrolizumab for platinum- and cetuximab-refractory head and neck cancer: results from a single-arm, phase II study. *J Clin Oncol*. 2017;35:1542-1549.
10. Mehra R, Seiwert TY, Gupta S, et al. Efficacy and safety of pembrolizumab in recurrent/metastatic head and neck squamous cell carcinoma: pooled analyses after long-term follow-up in KEYNOTE-012. *Br J Cancer*. 2018;119:153-159.
11. Cohen EEW, Soulières D, Le Tourneau C, et al. Pembrolizumab versus methotrexate, docetaxel, or cetuximab for recurrent or metastatic head-and-neck squamous cell carcinoma (KEYNOTE-040): a randomised, open-label, phase 3 study. *Lancet*. 2019;393:156-167.
12. Burtness B, Rischin D, Greil R, et al. Pembrolizumab alone or with chemotherapy for recurrent/metastatic head and neck squamous cell carcinoma in KEYNOTE-048: subgroup analysis by programmed death ligand-1 combined positive score. *J Clin Oncol*. 2022;40:2321-2332.
13. Gavrielatou N, Doumas S, Economopoulou P, Foukas PG, Psyrri A. Biomarkers for immunotherapy response in head and neck cancer. *Cancer Treat Rev*. 2020;84:101977.
14. Spector ME, Bellile E, Amlani L, et al. Prognostic value of tumor-infiltrating lymphocytes in head and neck squamous cell carcinoma. *JAMA Otolaryngol Head Neck Surg*. 2019;145:1012-1019.
15. Hanna GJ, Lizotte P, Cavanaugh M, et al. Frameshift events predict anti-PD-1/L1 response in head and neck cancer. *JCI Insight*. 2018;3:e98811.
16. Chen PL, Roh W, Reuben A, et al. Analysis of immune signatures in longitudinal tumor samples yields insight into biomarkers of response and mechanisms of resistance to immune checkpoint blockade. *Cancer Discov*. 2016;6:827-837.
17. Gavrielatou N, Vathiotis I, Aung TN, et al. Digital spatial profiling links beta-2-microglobulin expression with immune checkpoint blockade outcomes in head and neck squamous cell carcinoma. *Cancer Res Commun*. 2023;3:558-563.
18. Beechem JM. High-plex spatially resolved RNA and protein detection using digital spatial profiling: a technology designed for immuno-oncology biomarker discovery and translational research. *Methods Mol Biol*. 2020;2055:563-583.
19. Fang Z, Liu X, Peltz G. GSEApy: a comprehensive package for performing gene set enrichment analysis in Python. *Bioinformatics*. 2023;39:btac757.
20. Cabrita R, Lauss M, Sanna A, et al. Tertiary lymphoid structures improve immunotherapy and survival in melanoma. *Nature*. 2020;577:561-565.
21. Budczies J, Kirchner M, Kluck K, et al. A gene expression signature associated with B cells predicts benefit from immune checkpoint blockade in lung adenocarcinoma. *Oncoimmunology*. 2021;10:1860586.
22. Ju G, Yao Z, Zhao Y, Zhao X, Liu F. Data mining on identifying diagnosis and prognosis biomarkers in head and neck squamous carcinoma. *Sci Rep*. 2023;13:10020.
23. Kim SS, Shen S, Miyauchi S, et al. B cells improve overall survival in HPV-associated squamous cell carcinomas and are activated by radiation and PD-1 blockade. *Clin Cancer Res*. 2020;26:3345-3359.
24. Kuba K, Inoue H, Matsumura S, et al. A retrospective analysis of tumor infiltrating lymphocytes in head and neck squamous cell carcinoma patients treated with nivolumab. *Sci Rep*. 2022;12:22557.
25. Liu Y-T, Sun Z-J. Turning cold tumors into hot tumors by improving T-cell infiltration. *Theranostics*. 2021;11:5365-5386.
26. Clifton GT, Rothenberg M, Ascierto PA, et al. Developing a definition of immune exclusion in cancer: results of a modified Delphi workshop. *J Immunother Cancer*. 2023;11:e006773.
27. Chen DS, Mellman I. Elements of cancer immunity and the cancer-immune set point. *Nature*. 2017;541:321-330.
28. Miller BC, Sen DR, Al Abosy R, et al. Subsets of exhausted CD8+ T cells differentially mediate tumor control and respond to checkpoint blockade. *Nat Immunol*. 2019;20:326-336.
29. Nguyen N, Bellile E, Thomas D, et al. Tumor infiltrating lymphocytes and survival in patients with head and neck squamous cell carcinoma. *Head Neck*. 2016;38:1074-1084.
30. Balermpas P, Michel Y, Wagenblast J, et al. Tumour-infiltrating lymphocytes predict response to definitive chemoradiotherapy in head and neck cancer. *Br J Cancer*. 2014;110:501-509.
31. van Kempen PM, Noorlag R, Swartz JE, et al. Oropharyngeal squamous cell carcinomas differentially express granzyme inhibitors. *Cancer Immunol Immunother*. 2016;65:575-585.
32. Oguejiofor K, Hall J, Slater C, et al. Stromal infiltration of CD8 T cells is associated with improved clinical outcome in HPV-positive oropharyngeal squamous carcinoma. *Br J Cancer*. 2015;113:886-893.
33. Balermpas P, Rödel F, Rödel C, et al. CD8+ tumour-infiltrating lymphocytes in relation to HPV status and clinical outcome in patients with head and neck cancer after postoperative chemoradiotherapy: a multicentre study of the German cancer consortium radiation oncology group (DKTK-ROG). *Int J Cancer*. 2016;138:171-181.
34. Wang J, Tian S, Sun J, Zhang J, Lin L, Hu C. The presence of tumour-infiltrating lymphocytes (TILs) and the ratios between different subsets serve as prognostic factors in advanced hypopharyngeal squamous cell carcinoma. *BMC Cancer*. 2020;20:731.
35. Wouters MCA, Nelson BH. Prognostic significance of tumor-infiltrating B cells and plasma cells in human cancer. *Clin Cancer Res*. 2018;24:6125-6135.
36. Gavrielatou N, Vathiotis I, Economopoulou P, Psyrri A. The role of B cells in head and neck cancer. *Cancers (Basel)*. 2021;13:5383.
37. Helmink BA, Reddy SM, Gao J, et al. B cells and tertiary lymphoid structures promote immunotherapy response. *Nature*. 2020;577:549-555.
38. Petitprez F, de Reyniès A, Keung EZ, et al. B cells are associated with survival and immunotherapy response in sarcoma. *Nature*. 2020;577:556-560.
39. Vanhersecke L, Brunet M, Guégan JP, et al. Mature tertiary lymphoid structures predict immune checkpoint inhibitor efficacy in solid tumors independently of PD-L1 expression. *Nat Cancer*. 2021;2:794-802.
40. Vanhersecke L, Bougouin A, Crombé A, et al. Standardized pathology screening of mature tertiary lymphoid structures in cancers. *Lab Invest*. 2023;103:100063.
41. Le X, Ferrarotto R, Wise-Draper T, Gillison M. Evolving role of immunotherapy in recurrent metastatic head and neck cancer. *J Natl Compr Canc Netw*. 2020;18:899-906.
42. Colbeck EJ, Ager A, Gallimore A, Jones GW. Tertiary lymphoid structures in cancer: drivers of antitumor immunity, immunosuppression, or bystander sentinels in disease? *Front Immunol*. 2017;8:1830.
43. Sarvaria A, Madrigal JA, Saudemont A. B cell regulation in cancer and anti-tumor immunity. *Cell Mol Immunol*. 2017;14:662-674.
44. Tsou P, Katayama H, Ostrin EJ, Hanash SM. The emerging role of B cells in tumor immunity. *Cancer Res*. 2016;76:5597-5601.
45. Sautès-Fridman C, Petitprez F, Calderaro J, Fridman WH. Tertiary lymphoid structures in the era of cancer immunotherapy. *Nat Rev Cancer*. 2019;19:307-325.
46. Wieland A, Patel MR, Cardenas MA, et al. Defining HPV-specific B cell responses in patients with head and neck cancer. *Nature*. 2021;597:274-278.
47. Ruffin AT, Cillo AR, Tabib T, et al. B cell signatures and tertiary lymphoid structures contribute to outcome in head and neck squamous cell carcinoma. *Nat Commun*. 2021;12:3349.
48. Gui S, O'Neill WQ, Teknos TN, Pan Q. Plasma cell marker, immunoglobulin J polypeptide, predicts early disease-specific mortality in HPV+ HNSCC. *J Immunother Cancer*. 2021;9:e001259.
49. Bagaev A, Kotlov N, Nomie K, et al. Conserved pan-cancer microenvironment subtypes predict response to immunotherapy. *Cancer Cell*. 2021;39:845-865.e847.
50. Glencer AC, Wong JM, Hylton NM, et al. Modulation of the immune microenvironment of high-risk ductal carcinoma in situ by intralesional pembrolizumab injection. *NPJ Breast Cancer*. 2021;7:59.
51. Hamid O, Schmidt H, Nissan A, et al. A prospective phase II trial exploring the association between tumor microenvironment biomarkers and clinical activity of ipilimumab in advanced melanoma. *J Transl Med*. 2011;9:204.